

Mohamed Khider University of Biskra Faculty of exact sciences Department of Matter Sciences

MASTER MEMORY

Sciences of matter
Chemistry
Science of pharmaceutical chemistry

Réf.:

Presented by: **Ouamane Rayane**

THE:

In silico study of bioactive peptides as proteasome inhibitors

Jury: Ouassaf Mebarka Mohamed Khider University of Biskra Dr S.L.A President Mohamed Khider University of Biskra Dr Benbrahim Imane S.L.B Supervisor Dr Kenouch Samir S.L.A Mohamed Khider University of Biskra Examiner

Academic Year: 2024-2025

Acknowledgments

First and foremost, I would like to express my sincere gratitude to everyone who contributed, directly or indirectly, to the completion of this thesis.

I am especially grateful to my supervisor, Dr Benbrahim Imane, for their guidance, availability, and valuable support throughout this work.

I would also like to extend my heartfelt thanks to the members of the jury Dr Ouassaf Mebarka and Dr Kenouch Samir for taking the time to evaluate my work and for the interest they have shown in my research.

Many thanks as well to my professors and fellow students for their support, and the enriching discussions we shared during this journey.

Finally, I am deeply thankful to my family and loved ones for their encouragement, patience, and presence, which gave me the strength to carry on.

To all of you, thank you from the bottom of my heart.

Table of contents

List of tables	
List of figures	
List of abbreviations	
GENERAL INTRODUCTION	
General introduction	2
Bibliography	4
CHAPTER I: Biological activity of peptide Proline-Boronic acids as proteasome inhibitors	
1. Introduction to the proteasome and its inhibitors	6
1.1. Proteasome inhibitors in cancer therapy	6
2. Boronic acids as proteasome inhibitors	7
3. Advances in peptide and proline-boronic acids	8
4. Structural basis for proteasome inhibition	9
5. Conclusion and future perspective	10
Bibliography	11
CHAPTER II: Theoretical perspective and computational methods	
1. Theoretical background	16
1.1 Molecular modeling	16
1.2 Optimization in Molecular Modeling	16
1.3 Molecular Mechanics and Force Fields	16
1.4 Theoretical basis of molecular docking and AutoDock 4	17
1.5 Structure-based virtual screening	18
2. Computational workflow	18
2.1 Ligand preparation	18
2.2 Protein preparation	20
2.3 Docking protocol	20
2.4 Summary and outlook toward results	21
Bibliography	22
CHAPTER III: Results and discussion	
1. Validation of the docking protocol	27

1.1. Common interactions and binding features
1.2 Key differences and structural implications
2. Interpretation of docking results
2.1. Binding energy (ΔG)
2.2. Inhibition constant (Ki)
2.3. Ranking and activity profiles
2.3.1. Top-performing inhibitors
2.3.2. Moderate inhibitors
2.3.3. Weak inhibitors
3. Comparative analysis of ligand-protein interactions
3.1. Inhibitor I4: Optimal binding profile
3.2. Inhibitor I5: Strong binding but suboptimal orientation
3.3. Inhibitor II9: Unique Pi-Cation interaction but moderate binding
3.4. Inhibitor I6: Weaker binding and steric clashes
4. Structural and conformational analysis of ligands
5. Implications for inhibitor optimization
Bibliography
GENERAL CONCLUSION
Genaral conclusion
Abstract
Résumé

List of tables

Table 01: Molecular docking results.	30
Table 02: Summary of key insights	37
List of figures	
Chapter I	
Figure I.1: The cycle of ubiquitin-proteasome pathway	6
Figure I.2: Molecular structures of Bortezomib.	7
Figure I.3: Boronic acids equilibrium	8
Figure I.4: Peptide boronic acid analogues	9
Figure I.5: Proline-boronic acid optimized inhibitor.	9
Figure I.6: Yeast proteasome structure.	10
Chapter II	
Figure II.1: Molecular docking concept of ligand binding inside target site pocket	18
Figure II.2: Dipeptide proline-boronic acids series by Han et al	19
Figure II.3: Tripeptide proline-boronic acids series by Han et al.	19
Figure II.4: The prepared chain K of the 2F16 belonging to the yeast 20S proteasome struct	ture 20
Chapter III	
Figure III.1: Ligand co-crystallized	27
Figure III.2: Docked co-crystallized ligand interaction (left) and Experimental co-crystalliz	zed
ligand interaction (right)	28
Figure III.3: Interactions of ligand I4	32
Figure III.4: Interactions of ligand I5	33
Figure III.5: Interactions of ligand II9	33
Figure III.6: Interactions of ligand I6	34
Figure III.7: Superposition of the top performing ligands	38

List of abbreviations

AMBER: Assisted Model Building with Energy Refinement

ATP: Adenosine Triphosphate

EQ: Equation

FDA: Food and Drug Administration

H-Bonds: Hydrogen Bonds

HL-60: Human promyelocytic leukemia cell line

IC50: Inhibitory concentration 50

Ki: Inhibitor constant

LGA: Lamarckian Genetic Algorithm

MD: Molecular Dynamics

MDA-MB-231: A specific type of human breast cancer cell line.

MM+: Molecular Mechanics/Potential +

NF-κB: Nuclear Factor kappa-light-chain-enhancer of activated B cells

PDB: Protein Data Bank

PDBQT: Protein Data Bank Charges Torsions

RMSD: Root Mean Square Deviation

 ΔG : Binding free energy

SBVS: Structure-Based Virtual Screening

SAR: Structure Activity Relationship

UPS: Ubiquitin-Proteasome System

Amino Acids:

ALA: Alanine

ARG: Arginine

GLY: Glycine

LYS: Lysine

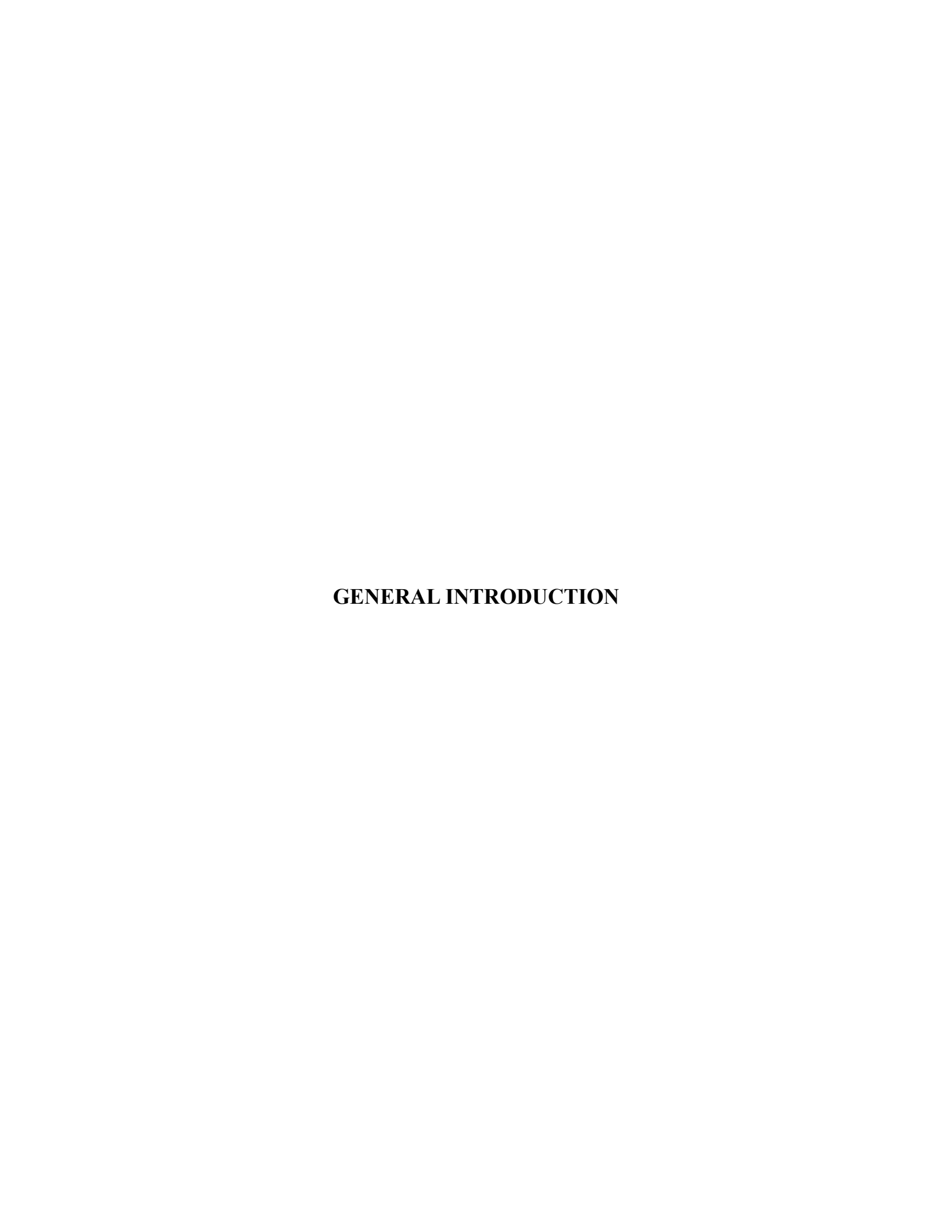
MET: Methionine

SER: Serine

THR: Threonine

TYR: Tyrosine

VAL: Valine



General introduction

The ubiquitin-proteasome system (UPS) is a central regulatory mechanism responsible for protein degradation and turnover within the cell. It plays a critical role in maintaining cellular homeostasis by modulating key processes such as the cell cycle, apoptosis, and stress response [1]. The 26S proteasome, a multicatalytic complex within the UPS, has emerged as a prominent therapeutic target for treating various diseases, particularly cancer [2].

Proteasome inhibitors like bortezomib have demonstrated substantial clinical efficacy; however, their application is often hindered by adverse effects and resistance development [3, 4]. Consequently, there is growing interest in the identification of novel bioactive compounds, particularly natural or synthetic peptides, with the potential to modulate proteasome activity more selectively and effectively [5, 6].

In the early stages of drug discovery, in silico techniques such as molecular docking provide a rapid and cost-effective means of predicting protein-ligand interactions and estimating binding affinities [5]. Docking software such as AutoDock can simulate the binding of peptides to the proteasome active site by evaluating the free energy of binding (ΔG) and the molecular interactions involved [7].

Molecular docking is particularly valuable in the pre-selection of lead compounds, allowing researchers to identify potential inhibitors based on their predicted binding affinity before proceeding to more costly experimental assays. Additionally, comparative docking studies against a co-crystallized ligand can further validate the binding poses and interaction profiles, providing insights into potential structural modifications to improve potency and selectivity [8].

The objective of this study is to apply molecular docking techniques to evaluate the inhibitory potential of selected bioactive peptides against the proteasome. Specifically, the study aims to:

- Assess the binding affinities and interaction profiles of the peptides using AutoDock.
- Compare docking results with existing experimental data to identify favorable conformations and key interaction patterns.

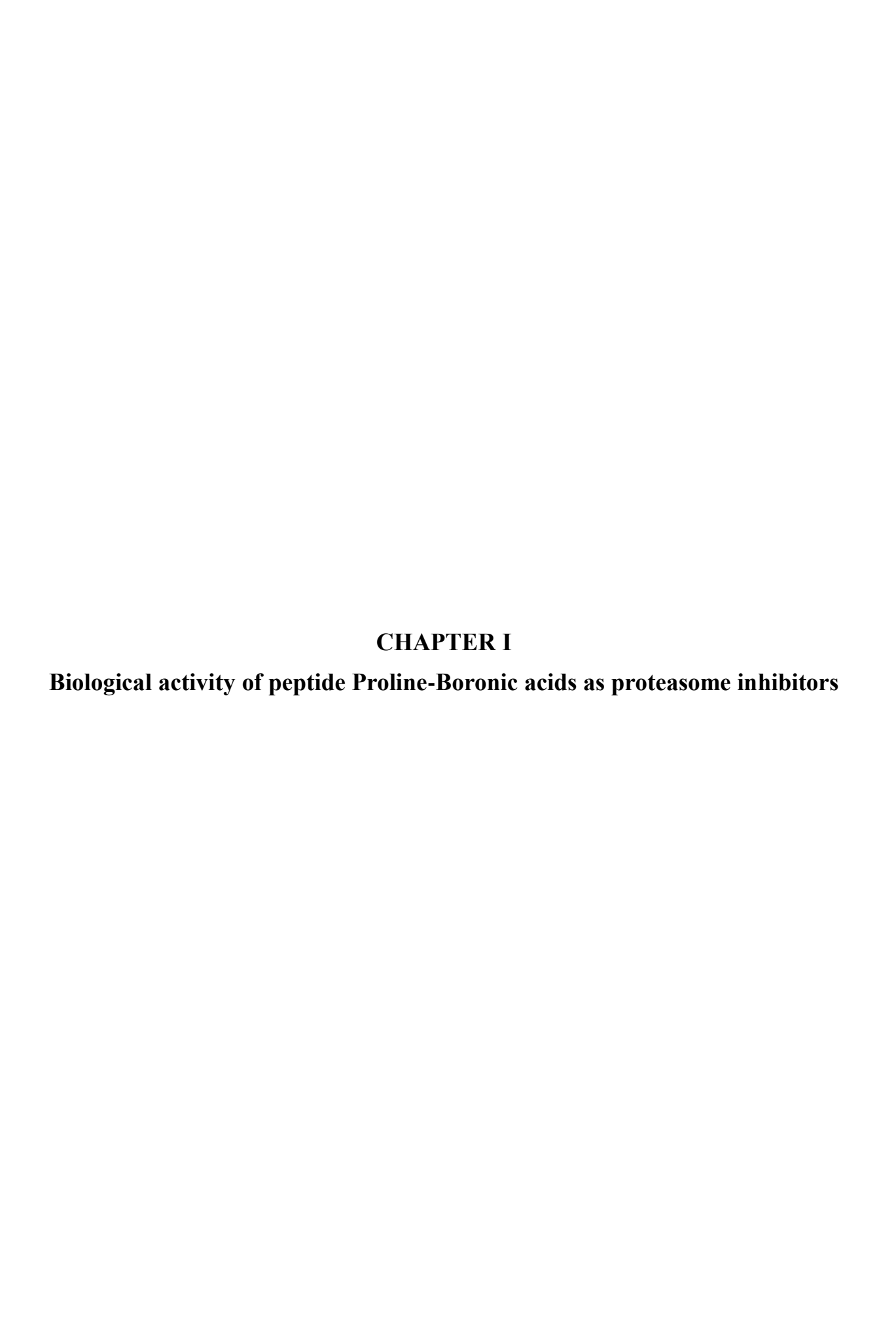
General introduction

• Propose structural modifications that could enhance the binding affinity or selectivity of promising inhibitors, particularly by targeting crucial residues such as TYR168, THR1, and GLY47.

By integrating in silico docking analysis with structure-based optimization strategies, this research seeks to contribute to the development of new peptide-based proteasome inhibitors that are more effective and potentially less toxic than existing therapeutic agents [3, 4].

Bibliography

- [1] Hershko, A., & Ciechanover, A. (1998). The ubiquitin system. Annual Review of Biochemistry, 67(1), 425–479. https://doi.org/10.1146/annurev.biochem.67.1.425
- [2] Adams, J. (2004). The proteasome: A suitable antineoplastic target. Nature Reviews Cancer, 4(5), 349–360. https://doi.org/10.1038/nrc1361
- [3] Adams, J., Palombella, V. J., & Elliott, P. J. (1999). Proteasome inhibition: A new strategy in cancer treatment. Investigational New Drugs, 1(4), 361–373. https://doi.org/10.1023/A:1006389720924
- [4] Richardson, P. G., Mitsiades, C., Hideshima, T., & Anderson, K. C. (2005). Proteasome inhibition in the treatment of cancer. Cell Cycle, 4(2), 290–296. https://doi.org/10.4161/cc.4.2.1411
- [5] Kitchen, D. B., Decornez, H., Furr, J. R., & Bajorath, J. (2004). Docking and scoring in virtual screening for drug discovery: Methods and applications. Nature Reviews Drug Discovery, 3(11), 935–949. https://doi.org/10.1038/nrd1549
- [6] Leach, A. R. (2001). Molecular modelling: Principles and applications (2nd ed.). Pearson Education.
- [7] Morris, G. M., Huey, R., Lindstrom, W., Sanner, M. F., Belew, R. K., Goodsell, D. S., & Olson, A. J. (2009). AutoDock4 and AutoDockTools4: Automated docking with selective receptor flexibility. Journal of Computational Chemistry, 30(16), 2785–2791. https://doi.org/10.1002/jcc.21256
- [8] Groll, M., Ditzel, L., Löwe, J., Stock, D., Bochtler, M., Bartunik, H. D., & Huber, R. (1997). Structure of 20S proteasome from yeast at 2.4 Å resolution. Nature, 386(6624), 463–471. https://doi.org/10.1038/386463a0



1. Introduction to the proteasome and its inhibitors

The proteasome is a large, ATP-dependent protein complex responsible for intracellular protein degradation. Proteins destined for destruction are first tagged with a polyubiquitin chain, a process mediated by E1 (activating), E2 (conjugating), and E3 (ligating) enzymes [1, 2].

The polyubiquitinated proteins are then recognized and degraded by the proteasome into small peptides, thus regulating crucial cellular functions such as cell-cycle progression and apoptosis.

[3]

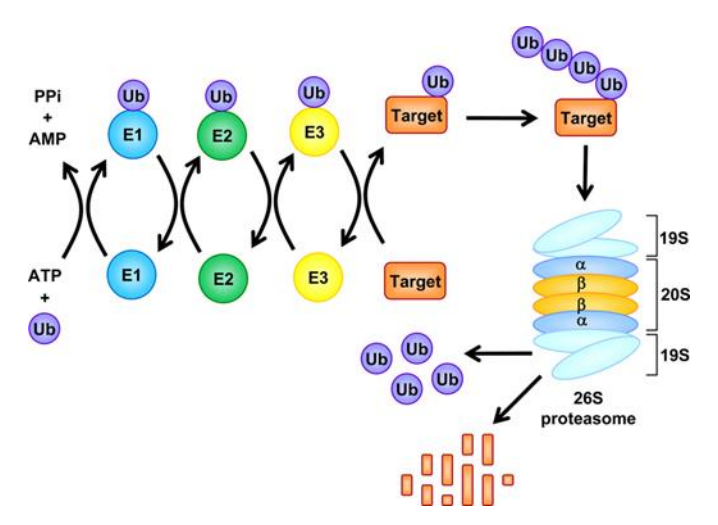


Figure I.1: The cycle of ubiquitin-proteasome pathway [4]

1.1. Proteasome inhibitors in cancer therapy

The idea of inhibiting the proteasome for therapeutic purposes was initially met with skepticism due to its essential cellular role [5]. However, early studies demonstrated that cancer cells are particularly sensitive to proteasome inhibition, leading to the development of new anticancer strategies [6].

Bortezomib (Velcade) became the first FDA-approved proteasome inhibitor, treating relapsed/refractory multiple myeloma and mantle cell lymphoma. By blocking the proteasome's chymotrypsin-like β 5 subunit, bortezomib prevents the degradation of pro-apoptotic proteins, thereby inducing cancer cell death. Clinical trials confirmed its efficacy and manageable toxicity. [7, 8]

Following bortezomib, Carfilzomib (Kyprolis), an irreversible inhibitor targeting the 20S proteasome, was developed. Approved for relapsed/refractory multiple myeloma, Carfilzomib showed increased specificity and therapeutic potential, especially in combination therapies. [9]

Later, Ixazomib (Ninlaro) emerged as the first oral proteasome inhibitor [10], offering the advantage of patient convenience. Ixazomib inhibits the $\beta 5$ subunit reversibly, inducing apoptosis in multiple myeloma cells and disrupting the tumor-supportive bone marrow microenvironment by inhibiting NF- κB signaling. [11, 12]

These inhibitors demonstrated that targeting the ubiquitin-proteasome system is a valid and effective anticancer strategy.

Figure I.2: Molecular structures of Bortezomib.

2. Boronic acids as proteasome inhibitors

Boronic acids, first synthesized by Edward Frankland in 1860 [13], are versatile organic molecules notable for their stability, low toxicity [14-16], and green degradation profile into boric acid [17, 18]. Their chemical properties, particularly their acid-base behavior depending on substituents, make them excellent bioisosteres of carboxylic acids. [14]

(a)
$$R-B$$
 + H_2O PKa $R-B^-OH$ + H_3O^+

(b)
$$R-B$$
 + H_2O PKa $R-B$ + H_3O^+

Figure I.3: Boronic acids equilibrium

In medicinal chemistry, boronic acids are uniquely suited for targeting the proteasome, particularly due to their ability to form reversible covalent bonds with the catalytic threonine residue of the proteasome's β subunits. [19]

Bortezomib exemplifies this mechanism, where its boronic acid moiety binds to THR1 of the β5 subunit, forming a tetrahedral intermediate that inhibits proteolysis. Its high affinity for \$5\$ explains its selectivity and potency, while weaker interactions with \beta1 and \beta2 reduce off-target effects. [20-22]

3. Advances in peptide and proline-boronic acids

Efforts to optimize proteasome inhibition led to the design of peptidomimetic boronic acids that mimic natural peptide substrates. These compounds aim to maintain high β5 selectivity while minimizing side effects. [23]

Proline-boronic acids, a newer subclass, offer improved pharmacological profiles over traditional peptide boronic acids. Research by Han et al, showed proline-boronic analogs with IC50 values below 10 nM against cancer cell lines like MDA-MB-231 and HL-60, demonstrating comparable or superior potency to bortezomib. [24] Such compounds exhibit promising therapeutic profiles, with high selectivity toward the β5 subunit and potentially lower toxicity, opening avenues for next-generation proteasome inhibitors. [25, 26]

Figure I.4: Peptide boronic acid analogues [23].

Figure I.5: Proline-boronic acid optimized inhibitor. [24]

4. Structural basis for proteasome inhibition

The 20S proteasome comprises four stacked heptameric rings in an $\alpha_7\beta_7\beta_7\alpha_7$ arrangement, forming a proteolytic chamber [27]. The catalytic activity resides in three β subunits:

- β1: Caspase-like, cleaves after acidic residues. [28]
- β2: Trypsin-like, cleaves after basic residues. [28]
- β5: Chymotrypsin-like, cleaves after hydrophobic residues. [21]

Inhibitors like bortezomib and ixazomib selectively target β 5 due to its hydrophobic S1 pocket. Bortezomib's boronic acid moiety binds THR1 hydroxyl groups [29], while its phenyl group fits tightly into the β 5 P1 hydrophobic pocket, stabilizing the inhibitory complex [30].

Crystallographic studies (PDB: 2F16) confirmed bortezomib's tight binding mode and explained its potent inhibition (Ki for β 5 = 0.6 nM), highlighting the importance of rational drug design targeting the chymotrypsin-like subunit. [30, 31]

In this study, the $\beta 5$ subunit was selected as the target for docking analysis, as it plays a crucial role in proteasome function. The proteasome structure contains two $\beta 5$ subunits, represented as chain K and chain Y in the PDB databank. Since both chains are structurally identical, chain K was chosen for the docking analysis to avoid redundancy and streamline computational analysis.

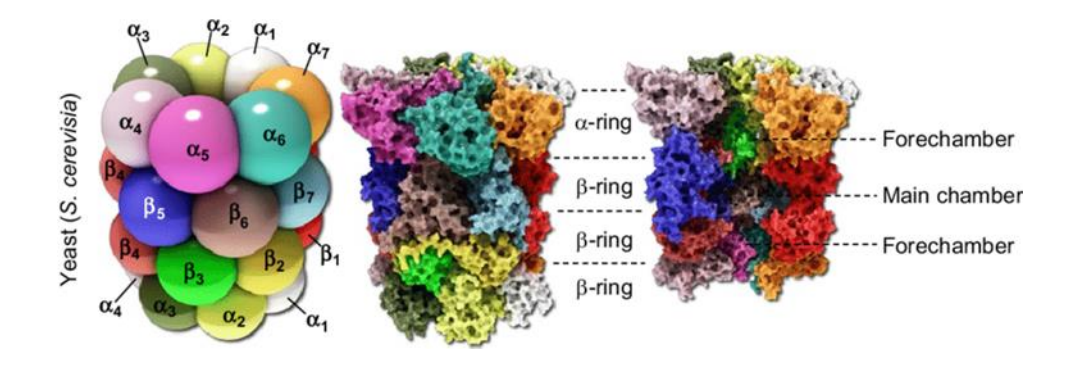


Figure I.6: Yeast proteasome structure.

5. Conclusion and future perspective

The successful targeting of the proteasome by boronic acid-based inhibitors has transformed the treatment of multiple myeloma and other malignancies. Advances in peptide and proline-boronic acid chemistry offer even more selective and potent inhibitors, with the promise of reduced side effects.

Future drug discovery efforts should focus on maintaining strong $\beta 5$ inhibition while minimizing toxicity, shortening development times, and improving patient outcomes.

This work aims to valorize selected peptide boronic acid analogues through computational optimization protocols dedicated to enhancing 20S proteasome inhibition selectivity and efficiency.

Bibliography

- [1] A. Hershko, A. Ciechanover, THE UBIQUITIN SYSTEM, Annu. Rev. Biochem. 67 (1998) 425–479. https://doi.org/10.1146/annurev.biochem.67.1.425.
- [2] T. Ravid, M. Hochstrasser, Diversity of degradation signals in the ubiquitin–proteasome system, Nat Rev Mol Cell Biol 9 (2008) 679–689. https://doi.org/10.1038/nrm2468.
- [3] H.-C. Tai, E.M. Schuman, Ubiquitin, the proteasome and protein degradation in neuronal function and dysfunction, Nat Rev Neurosci 9 (2008) 826–838. https://doi.org/10.1038/nrn2499.
- [4] H. Yang, K. Landis-Piwowar, D. Chen, V. Milacic, Q. Dou, Natural Compounds with Proteasome Inhibitory Activity for Cancer Prevention and Treatment, CPPS 9 (2008) 227–239. https://doi.org/10.2174/138920308784533998.
- [5] R.Z. Orlowski, J.R. Eswara, A. Lafond-Walker, M.R. Grever, M. Orlowski, C.V. Dang, Tumor growth inhibition induced in a murine model of human Burkitt's lymphoma by a proteasome inhibitor, Cancer Research 58 (1998) 4342–4348.
- [6] J. Adams, V.J. Palombella, E.A. Sausville, J. Johnson, A. Destree, D.D. Lazarus, J. Maas, C.S. Pien, S. Prakash, P.J. Elliott, Proteasome inhibitors: a novel class of potent and effective antitumor agents, Cancer Research 59 (1999) 2615–2622.
- [7] R.C. Kane, P.F. Bross, A.T. Farrell, R. Pazdur, Velcade®: U.S. FDA Approval for the Treatment of Multiple Myeloma Progressing on Prior Therapy, The Oncologist 8 (2003) 508–513. https://doi.org/10.1634/theoncologist.8-6-508.
- [8] R.C. Kane, R. Dagher, A. Farrell, C.-W. Ko, R. Sridhara, R. Justice, R. Pazdur, Bortezomib for the Treatment of Mantle Cell Lymphoma, Clinical Cancer Research 13 (2007) 5291–5294. https://doi.org/10.1158/1078-0432.CCR-07-0871.
- [9] S. Richard, S. Jagannath, H.J. Cho, S. Parekh, D. Madduri, J. Richter, A. Chari, A comprehensive overview of daratumumab and carfilzomib and the recently approved daratumumab, carfilzomib and dexamethasone regimen in relapsed/refractory multiple myeloma, Expert Review of Hematology 14 (2021) 31–45. https://doi.org/10.1080/17474086.2021.1858790.
- [10] J. Xie, N. Wan, Z. Liang, T. Zhang, J. Jiang, Ixazomib the first oral proteasome inhibitor, Leukemia & Lymphoma 60 (2019) 610–618. https://doi.org/10.1080/10428194.2018.1523398.

- [11] D. Chauhan, Z. Tian, B. Zhou, D. Kuhn, R. Orlowski, N. Raje, P. Richardson, K.C. Anderson, *In Vitro* and *In Vivo* Selective Antitumor Activity of a Novel Orally Bioavailable Proteasome Inhibitor MLN9708 against Multiple Myeloma Cells, Clinical Cancer Research 17 (2011) 5311–5321. https://doi.org/10.1158/1078-0432.CCR-11-0476.
- [12] D.J. Kuhn, R.Z. Orlowski, The Immunoproteasome as a Target in Hematologic Malignancies, Seminars in Hematology 49 (2012) 258–262. https://doi.org/10.1053/j.seminhematol.2012.04.003.
- [13] E. Frankland, B.F. Duppa, Vorläufige Notiz über Boräthyl, Justus Liebigs Ann. Chem. 115 (1860) 319–322. https://doi.org/10.1002/jlac.18601150324.
- [14] P.C. Trippier, C. McGuigan, Boronic acids in medicinal chemistry: anticancer, antibacterial and antiviral applications, Med. Chem. Commun. 1 (2010) 183. https://doi.org/10.1039/c0md00119h.
- [15] J.N. Cambre, B.S. Sumerlin, Biomedical applications of boronic acid polymers, Polymer 52 (2011) 4631–4643. https://doi.org/10.1016/j.polymer.2011.07.057.
- [16] W.L.A. Brooks, B.S. Sumerlin, Synthesis and Applications of Boronic Acid-Containing Polymers: From Materials to Medicine, Chem. Rev. 116 (2016) 1375–1397. https://doi.org/10.1021/acs.chemrev.5b00300.
- [17] N.A. Petasis, Expanding Roles for Organoboron Compounds Versatile and Valuable Molecules for Synthetic, Biological and Medicinal Chemistry, Aust. J. Chem. 60 (2007) 795. https://doi.org/10.1071/CH07360.
- [18] S.J. Baker, C.Z. Ding, T. Akama, Y.-K. Zhang, V. Hernandez, Y. Xia, Therapeutic Potential of Boron-Containing Compounds, Future Med. Chem. 1 (2009) 1275–1288. https://doi.org/10.4155/fmc.09.71.
- [19] M. Groll, L. Ditzel, J. Löwe, D. Stock, M. Bochtler, H.D. Bartunik, R. Huber, Structure of 20S proteasome from yeast at 2.4Å resolution, Nature 386 (1997) 463–471. https://doi.org/10.1038/386463a0.
- [20] J. Adams, The proteasome: structure, function, and role in the cell, Cancer Treatment Reviews 29 (2003) 3–9. https://doi.org/10.1016/S0305-7372(03)00081-1.
- [21] L. Borissenko, M. Groll, 20S Proteasome and Its Inhibitors: Crystallographic Knowledge for Drug Development, Chem. Rev. 107 (2007) 687–717. https://doi.org/10.1021/cr0502504.

- [22] A.F. Kisselev, W.A. van der Linden, H.S. Overkleeft, Proteasome Inhibitors: An Expanding Army Attacking a Unique Target, Chemistry & Biology 19 (2012) 99–115. https://doi.org/10.1016/j.chembiol.2012.01.003.
- [23] K. Scarbaci, V. Troiano, R. Ettari, A. Pinto, N. Micale, C. Di Giovanni, C. Cerchia, T. Schirmeister, E. Novellino, A. Lavecchia, M. Zappalà, S. Grasso, Development of Novel Selective Peptidomimetics Containing a Boronic Acid Moiety, Targeting the 20S Proteasome as Anticancer Agents, ChemMedChem 9 (2014) 1801–1816. https://doi.org/10.1002/cmdc.201402075.
- [24] L. Han, Y. Wen, R. Li, B. Xu, Z. Ge, X. Wang, T. Cheng, J. Cui, R. Li, Synthesis and biological activity of peptide proline-boronic acids as proteasome inhibitors, Bioorganic & Medicinal Chemistry 25 (2017) 4031–4044. https://doi.org/10.1016/j.bmc.2017.05.049.
- [25] M. Screen, M. Britton, S.L. Downey, M. Verdoes, M.J. Voges, A.E.M. Blom, P.P. Geurink, M.D.P. Risseeuw, B.I. Florea, W.A. Van Der Linden, A.A. Pletnev, H.S. Overkleeft, A.F. Kisselev, Nature of Pharmacophore Influences Active Site Specificity of Proteasome Inhibitors, Journal of Biological Chemistry 285 (2010) 40125–40134. https://doi.org/10.1074/jbc.M110.160606.
- [26] X. Zhang, A. Adwal, A.G. Turner, D.F. Callen, A.D. Abell, New Peptidomimetic Boronates for Selective Inhibition of the Chymotrypsin-like Activity of the 26S Proteasome, ACS Med. Chem. Lett. 7 (2016) 1039–1043. https://doi.org/10.1021/acsmedchemlett.6b00217.
- [27] O. Coux, K. Tanaka, A.L. Goldberg, STRUCTURE AND FUNCTIONS OF THE 20S AND 26S PROTEASOMES, Annu. Rev. Biochem. 65 (1996) 801–847. https://doi.org/10.1146/annurev.bi.65.070196.004101.
- [28] M. Groll, C.R. Berkers, H.L. Ploegh, H. Ovaa, Crystal Structure of the Boronic Acid-Based Proteasome Inhibitor Bortezomib in Complex with the Yeast 20S Proteasome, Structure 14 (2006) 451–456. https://doi.org/10.1016/j.str.2005.11.019.
- [29] E.M. Huber, M. Basler, R. Schwab, W. Heinemeyer, C.J. Kirk, M. Groettrup, M. Groll, Immuno- and Constitutive Proteasome Crystal Structures Reveal Differences in Substrate and Inhibitor Specificity, Cell 148 (2012) 727–738. https://doi.org/10.1016/j.cell.2011.12.030.

- [30] J. Schrader, F. Henneberg, R.A. Mata, K. Tittmann, T.R. Schneider, H. Stark, G. Bourenkov, A. Chari, The inhibition mechanism of human 20 S proteasomes enables next-generation inhibitor design, Science 353 (2016) 594–598. https://doi.org/10.1126/science.aaf8993.
- [31] E. Kupperman, E.C. Lee, Y. Cao, B. Bannerman, M. Fitzgerald, A. Berger, J. Yu, Y. Yang, P. Hales, F. Bruzzese, J. Liu, J. Blank, K. Garcia, C. Tsu, L. Dick, P. Fleming, L. Yu, M. Manfredi, M. Rolfe, J. Bolen, Evaluation of the Proteasome Inhibitor MLN9708 in Preclinical Models of Human Cancer, Cancer Research 70 (2010) 1970–1980. https://doi.org/10.1158/0008-5472.CAN-09-2766.

CHAPTER II

Theoretical perspective and computational methods

1. Theoretical background

1.1 Molecular modeling

Molecular modeling encompasses computational methods that simulate the structure, behavior, and interactions of molecular systems [1]. It bridges theoretical chemistry and computer science, enabling prediction and visualization of molecular properties through a range of approaches from simple physical models to sophisticated computer-generated simulations [2].

Key techniques include:

- Quantum mechanics: Modeling electronic structure [3].
- Molecular mechanics: Using force fields to simulate atomic interactions [2].
- Molecular dynamics: Simulations atomic movement over time [4].
- **Molecular docking:** Predicting binding affinities and conformations [5].

These methods allow researchers to explore reaction mechanisms, design materials, and develop pharmaceuticals efficiently [6].

1.2 Optimization in molecular modeling

Optimization is essential for finding molecular structures at their lowest energy states. Methods like: Steepest Descent [7], Fletcher-Reeves [8], and Polak-Ribière [9] allow systematic minimization of molecular energies by adjusting bond lengths, angles, and dihedrals. Optimization ensures structural stability and enables accurate property prediction.

1.3 Molecular mechanics and force fields

1.3.1 Molecular mechanics principles

Molecular mechanics models molecules without solving quantum equations. It treats atoms as balls and bonds as springs, using classical physics to calculate system energies [1, 3]. The total molecular energy is divided into contributions from bond stretching, angle bending, dihedral torsions, and non-bonded interactions [2, 10].

1.3.2 Force fields overview

Force fields like MM+ and AMBER define mathematical equations for:

- **Bond stretching** (Hooke's law model)
- Angle bending

- Dihedral rotation
- Van der waals interactions (Lennard-Jones potential)
- **Electrostatics** (Coulomb's law)
- **Hydrogen bonding** (specific to AMBER) [11–13].

Energy expressions:

$$E_{total} = E_{bonded} + E_{non-bonded}$$
 ... (eq. 01)
$$E_{bonded} = Bond \ Stretching + Angle \ Bending + Dihedrals \ ... \ (eq. 02)$$

$$E_{non-bonded} = Electrostatic + Van \ Der \ Waals \ ... \ (eq. 03)$$

1.3.3 Comparison between MM+ and AMBER

- MM+: Suited for general organic molecules; faster but less specialized [14–17].
- **AMBER**: Tailored for biomolecules like proteins and nucleic acids; more accurate for biological systems [18–24].

Both include similar energy terms but differ in parameterization depth and electrostatic models.

1.4 Theoretical basis of molecular docking and AutoDock 4

Molecular docking predicts the preferred binding orientation of a ligand to a receptor, estimating the strength and nature of molecular interactions [25–27].

AutoDock 4 uses a semi-empirical scoring function combining:

- Van der Waals interactions,
- Hydrogen bonding,
- Electrostatic interactions,
- Desolvation effects [28,29].

For conformational search, AutoDock 4 employs the Lamarckian Genetic Algorithm (LGA) [30]:

- Global search via genetic mutations and crossover
- Local search via energy minimization.

This hybrid strategy enables efficient exploration of the vast conformational space, overcoming local minima, and ensuring robust docking predictions.

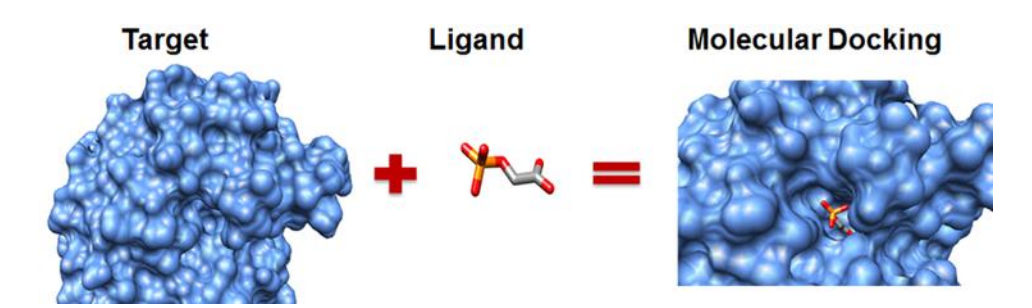


Figure II.1: Molecular docking concept of ligand binding inside target site pocket.

1.5 Structure-based virtual screening

Structure-Based Virtual Screening (SBVS) is a computational approach that identifies potential bioactive compounds by evaluating their predicted binding affinity to a known three-dimensional structure of a biological target [31–33].

In SBVS:

- A large set of ligands is virtually "docked" into the binding site.
- Each ligand is scored based on predicted binding energy and interaction patterns.
- Top candidates are prioritized for further experimental or computational investigation.

This approach is widely used in drug discovery, especially when high-resolution crystal structures or high-quality homology models are available [31].

In this study, SBVS was applied by docking a series of 17 dipeptide and tripeptide proline-boronic acids into the validated active site of the 20S proteasome structure (PDB ID: 2F16).

2. Computational workflow

2.1 Ligand preparation

Peptide proline-boronic acid ligands were selected based on the work of Han et al. [34]. Structures were optimized using HyperChem 7.0 [35], applying MM+ followed by AMBER force fields. Ligands were prepared for docking by assigning Gasteiger charges and defining rotatable bonds using AutoDock Tools.

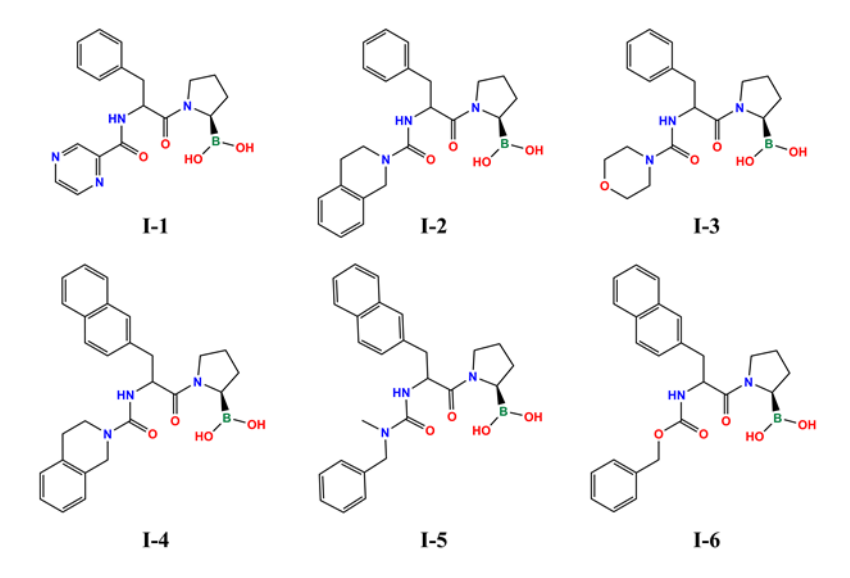


Figure II.2: Dipeptide proline-boronic acids series by Han et al. [34]

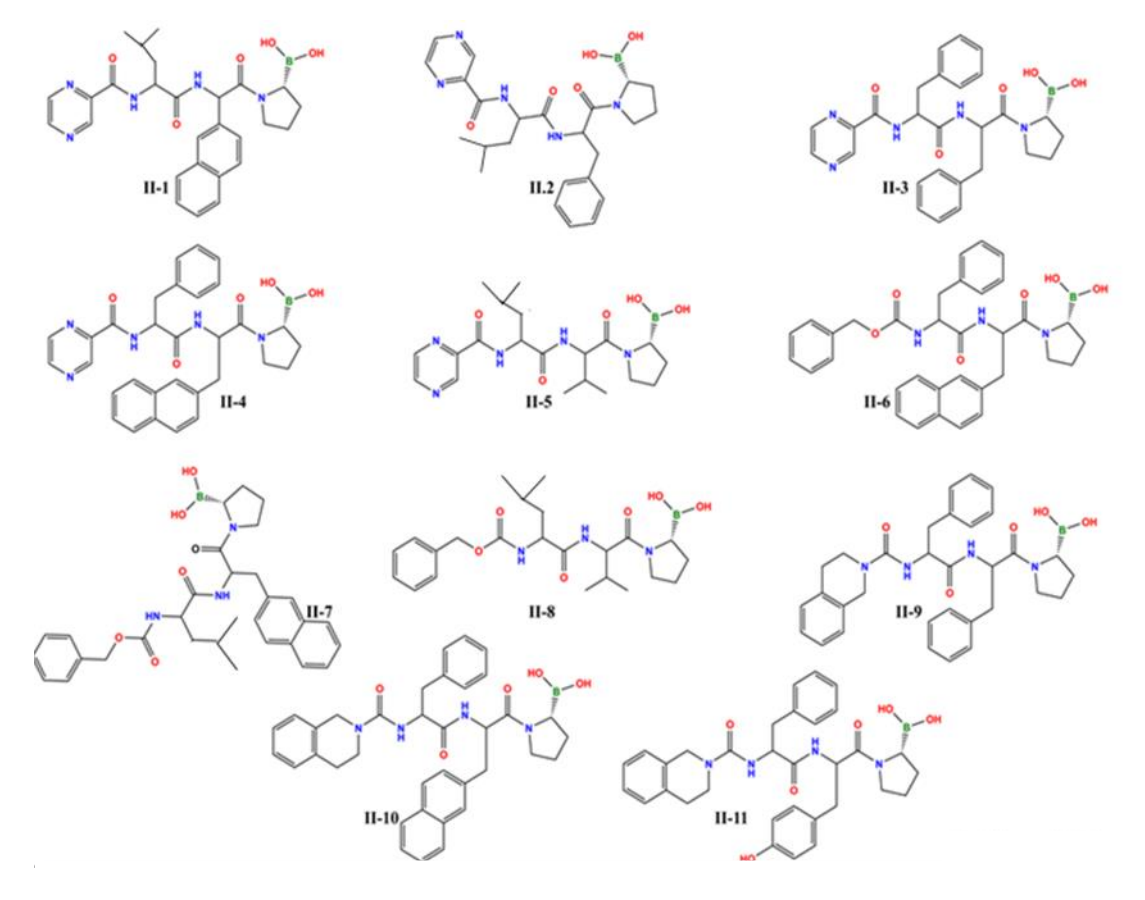


Figure II.3: Tripeptide proline-boronic acids series by Han et al. [34]

2.2 Protein preparation

The yeast 20S proteasome (PDB ID: 2F16) was selected as the target [36, 37]. Preparation steps included:

- Cleaning water molecules and unnecessary chains.
- Adding hydrogens and assigning Kollman charges.

Then identifying key residues (THR1 and MET45) within the active site that are likely to undergo conformational changes upon ligand binding. These residues were defined as flexible to better mimic the induced-fit effect and improve docking accuracy. The remaining part of the protein was treated as rigid to reduce computational cost while preserving the overall structural integrity. Flexible residues were selected based on proximity to the binding pocket, and previous literature or structural analysis.

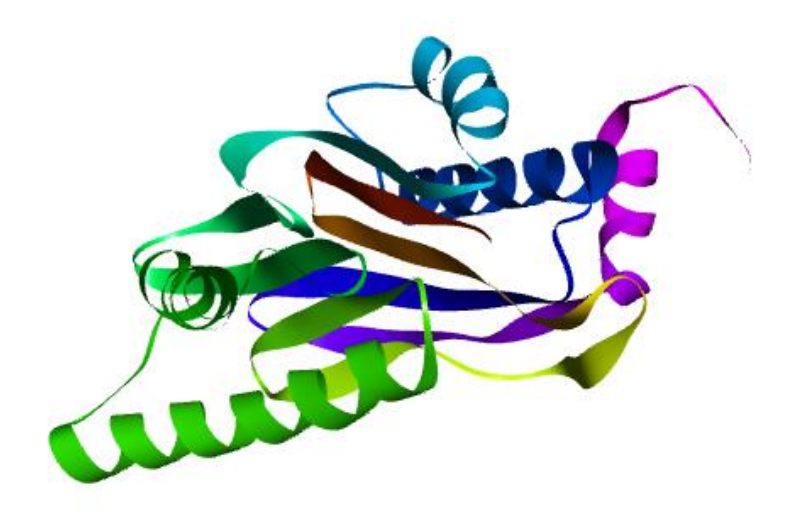


Figure II.4: The prepared chain K of the 2F16 belonging to the yeast 20S proteasome structure.

2.3 Docking protocol

The binding site was identified by analyzing the crystal structure and the binding mode of the cocrystallized ligand (bortezomib).

Based on this analysis, a grid box was carefully centered on the active site residues to perform a targeted docking approach, ensuring that docking simulations focused specifically on the biologically relevant pocket involved in proteasome inhibition

• Grid box size: 85 67 50

• Gridcenter: 11.163, -137.436, 13.876

AutoDock 4.2 was employed for docking simulations [28–39].

• Search method: Lamarckian Genetic Algorithm.

• Docking parameters: 10 runs, 150 population size, long evaluation count.

Editing docking and grid parameter files was necessary to incorporate boron atom types into the docking process.

2.4 Summary and outlook toward results

The molecular modeling strategies, optimization algorithms, force fields, and docking methodologies detailed in this chapter provided the computational foundation for our structure-based virtual screening approach.

Building upon the biological rationale established in Chapter I, the carefully prepared molecular systems and docking protocols described here enable the evaluation of peptide proline-boronic acid analogues as potential proteasome inhibitors.

The next chapter presents the results obtained from the virtual screening, redocking validation, and interaction analysis, followed by a critical discussion of the findings in the context of therapeutic development.

Bibliography

- [1] A.R. Leach, Molecular modelling: principles and applications, Pearson education, 2001.
- [2] T. Schlick, Molecular Modeling and Simulation: An Interdisciplinary Guide: An Interdisciplinary Guide, Springer New York, New York, NY, 2010. https://doi.org/10.1007/978-1-4419-6351-2.
- [3] F. Jensen, Introduction to computational chemistry, John wiley & sons, 2017.
- [4] D. Frenkel, B. Smit, Understanding molecular simulation: from algorithms to applications, Elsevier, 2023.
- [5] C.J. Cramer, Essentials of computational chemistry: theories and models, John Wiley & Sons, 2013.
- [6] The Modeling of Molecules Through Computational Methods, in: Computational Chemistry and Molecular Modeling, Springer Berlin Heidelberg, Berlin, Heidelberg, 2008: pp. 229–274. https://doi.org/10.1007/978-3-540-77304-7_12.
- [7] J.C. Meza, Steepest descent, WIREs Computational Stats 2 (2010) 719–722. https://doi.org/10.1002/wics.117.
- [8] L. Zhang, W. Zhou, D. Li, Global convergence of a modified Fletcher–Reeves conjugate gradient method with Armijo-type line search, Numer. Math. 104 (2006) 561–572. https://doi.org/10.1007/s00211-006-0028-z.
- [9] L. Grippo, S. Lucidi, A globally convergent version of the Polak-Ribière conjugate gradient method, Mathematical Programming 78 (1997) 375–391. https://doi.org/10.1007/BF02614362.
- [10] B.R. Brooks, R.E. Bruccoleri, B.D. Olafson, D.J. States, S. Swaminathan, M. Karplus, CHARMM: A program for macromolecular energy, minimization, and dynamics calculations, J Comput Chem 4 (1983) 187–217. https://doi.org/10.1002/jcc.540040211.
- [11] L. Monticelli, D.P. Tieleman, Force Fields for Classical Molecular Dynamics, in: L. Monticelli, E. Salonen (Eds.), Biomolecular Simulations, Humana Press, Totowa, NJ, 2013: pp. 197–213. https://doi.org/10.1007/978-1-62703-017-5_8.
- [12] K. Vanommeslaeghe, E. Hatcher, C. Acharya, S. Kundu, S. Zhong, J. Shim, E. Darian, O. Guvench, P. Lopes, I. Vorobyov, A.D. Mackerell, CHARMM general force field: A force field for drug-like molecules compatible with the CHARMM all-atom additive biological force fields, J Comput Chem 31 (2010) 671–690. https://doi.org/10.1002/jcc.21367.

- [13] K. Vanommeslaeghe, O. Guvench, A.D. MacKerell, Molecular Mechanics, CPD 20 (2014) 3281–3292. https://doi.org/10.2174/13816128113199990600.
- [14] J.W. Ponder, D.A. Case, Force Fields for Protein Simulations, in: Advances in Protein Chemistry, Elsevier, 2003: pp. 27–85. https://doi.org/10.1016/S0065-3233(03)66002-X.
- [15] T.E. Cheatham, P. Cieplak, P.A. Kollman, A Modified Version of the Cornell *et al.* Force Field with Improved Sugar Pucker Phases and Helical Repeat, Journal of Biomolecular Structure and Dynamics 16 (1999) 845–862. https://doi.org/10.1080/07391102.1999.10508297.
- [16] P. Cieplak, W.D. Cornell, C. Bayly, P.A. Kollman, Application of the multimolecule and multiconformational RESP methodology to biopolymers: Charge derivation for DNA, RNA, and proteins, J Comput Chem 16 (1995) 1357–1377. https://doi.org/10.1002/jcc.540161106.
- [17] N.L. Allinger, Conformational analysis. 130. MM2. A hydrocarbon force field utilizing V1 and V2 torsional terms, J. Am. Chem. Soc. 99 (1977) 8127–8134. https://doi.org/10.1021/ja00467a001.
- [18] S.J. Weiner, P.A. Kollman, D.A. Case, U.C. Singh, C. Ghio, G. Alagona, S. Profeta, P. Weiner, A new force field for molecular mechanical simulation of nucleic acids and proteins, J. Am. Chem. Soc. 106 (1984) 765–784. https://doi.org/10.1021/ja00315a051.
- [19] J. Wang, R.M. Wolf, J.W. Caldwell, P.A. Kollman, D.A. Case, Development and testing of a general amber force field, J Comput Chem 25 (2004) 1157–1174. https://doi.org/10.1002/jcc.20035.
- [20] V. Hornak, R. Abel, A. Okur, B. Strockbine, A. Roitberg, C. Simmerling, Comparison of multiple Amber force fields and development of improved protein backbone parameters, Proteins 65 (2006) 712–725. https://doi.org/10.1002/prot.21123.
- [21] D.A. Case, T.E. Cheatham, T. Darden, H. Gohlke, R. Luo, K.M. Merz, A. Onufriev, C. Simmerling, B. Wang, R.J. Woods, The Amber biomolecular simulation programs, J Comput Chem 26 (2005) 1668–1688. https://doi.org/10.1002/jcc.20290.
- [22] W.D. Cornell, P. Cieplak, C.I. Bayly, I.R. Gould, K.M. Merz, D.M. Ferguson, D.C. Spellmeyer, T. Fox, J.W. Caldwell, P.A. Kollman, A Second Generation Force Field for the Simulation of Proteins, Nucleic Acids, and Organic Molecules, J. Am. Chem. Soc. 117 (1995) 5179–5197. https://doi.org/10.1021/ja00124a002.

- [23] R. Salomon-Ferrer, D.A. Case, R.C. Walker, An overview of the Amber biomolecular simulation package, WIREs Comput Mol Sci 3 (2013) 198–210. https://doi.org/10.1002/wcms.1121.
- [24] J.A. Maier, C. Martinez, K. Kasavajhala, L. Wickstrom, K.E. Hauser, C. Simmerling, ff14SB: Improving the Accuracy of Protein Side Chain and Backbone Parameters from ff99SB, J. Chem. Theory Comput. 11 (2015) 3696–3713. https://doi.org/10.1021/acs.jctc.5b00255.
- [25] G.M. Morris, M. Lim-Wilby, Molecular Docking, in: A. Kukol (Ed.), Molecular Modeling of Proteins, Humana Press, Totowa, NJ, 2008: pp. 365–382. https://doi.org/10.1007/978-1-59745-177-2 19.
- [26] R.N. Sahoo, S. Pattanaik, G. Pattnaik, S. Mallick, R. Mohapatra, Review on the use of Molecular Docking as the First Line Tool in Drug Discovery and Development, IJPS 84 (2022). https://doi.org/10.36468/pharmaceutical-sciences.1031.
- [27] X.-Y. Meng, H.-X. Zhang, M. Mezei, M. Cui, Molecular Docking: A Powerful Approach for Structure-Based Drug Discovery, CAD 7 (2011) 146–157. https://doi.org/10.2174/157340911795677602.
- [28] G.M. Morris, D.S. Goodsell, R.S. Halliday, R. Huey, W.E. Hart, R.K. Belew, A.J. Olson, Automated docking using a Lamarckian genetic algorithm and an empirical binding free energy function, J. Comput. Chem. 19 (1998) 1639–1662. https://doi.org/10.1002/(SICI)1096-987X(19981115)19:14<1639::AID-JCC10>3.0.CO;2-B.
- [29] R. Huey, G.M. Morris, A.J. Olson, D.S. Goodsell, A semiempirical free energy force field with charge-based desolvation, J Comput Chem 28 (2007) 1145–1152. https://doi.org/10.1002/jcc.20634.
- [30] O. Trott, A.J. Olson, AutoDock Vina: Improving the speed and accuracy of docking with a new scoring function, efficient optimization, and multithreading, J Comput Chem 31 (2010) 455–461. https://doi.org/10.1002/jcc.21334.
- [31] P. Kolb, R.S. Ferreira, J.J. Irwin, B.K. Shoichet, Docking and chemoinformatic screens for new ligands and targets, Curr Opin Biotechnol 20 (2009) 429–436. https://doi.org/10.1016/j.copbio.2009.08.003.
- [32] P. Kolb, J.J. Irwin, Docking screens: right for the right reasons?, Curr Top Med Chem 9 (2009) 755–770. https://doi.org/10.2174/156802609789207091.

- [33] B.K. Shoichet, Virtual screening of chemical libraries, Nature 432 (2004) 862–865. https://doi.org/10.1038/nature03197.
- [34] L. Han, Y. Wen, R. Li, B. Xu, Z. Ge, X. Wang, T. Cheng, J. Cui, R. Li, Synthesis and biological activity of peptide proline-boronic acids as proteasome inhibitors, Bioorganic & Medicinal Chemistry 25 (2017) 4031–4044. https://doi.org/10.1016/j.bmc.2017.05.049.
- [35] HyperChem(TM) Professional, (n.d.). http://www.hypercubeusa.com/.
- [36] H.M. Berman, The Protein Data Bank, Nucleic Acids Research 28 (2000) 235–242. https://doi.org/10.1093/nar/28.1.235.
- [37] M. Groll, C.R. Berkers, H.L. Ploegh, H. Ovaa, Crystal Structure of the Boronic Acid-Based Proteasome Inhibitor Bortezomib in Complex with the Yeast 20S Proteasome, Structure 14 (2006) 451–456. https://doi.org/10.1016/j.str.2005.11.019.
- [38] G.M. Morris, R. Huey, W. Lindstrom, M.F. Sanner, R.K. Belew, D.S. Goodsell, A.J. Olson, AutoDock4 and AutoDockTools4: Automated docking with selective receptor flexibility, J Comput Chem 30 (2009) 2785–2791. https://doi.org/10.1002/jcc.21256.
- [39] S. Forli, R. Huey, M.E. Pique, M.F. Sanner, D.S. Goodsell, A.J. Olson, Computational protein–ligand docking and virtual drug screening with the AutoDock suite, Nat Protoc 11 (2016) 905–919. https://doi.org/10.1038/nprot.2016.051.

CHAPTER III

Results and discussion

Chapter III Results and discussion

1. Validation of the docking protocol

Before analyzing the results of the virtual screening, it was critical to validate the docking methodology to ensure the reliability of the predicted binding poses. This was achieved through a self-docking (re-docking) approach, where in the native co-crystallized ligand of the proteasome was extracted and re-docked into its original binding site using the same docking parameters as applied to the test compounds.

The predicted pose was then compared to the experimentally resolved pose by calculating the root-mean-square deviation (RMSD) between the two structures. Using AutoDock Tools, an RMSD of 2.976 Å was obtained as shown in figure III.1.

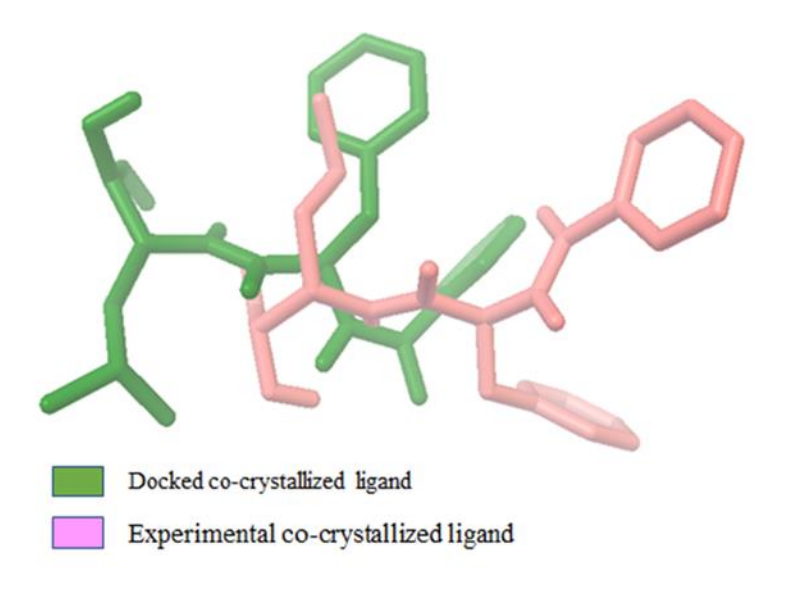


Figure III.1: Ligand co-crystallized

Although lower RMSD values—particularly those under **2.0** Å— are generally considered ideal, several studies support that RMSD values below **3.0** Å are still within the acceptable range for docking validation, especially when considering ligand or protein flexibility [1-3]. RMSD values in the **2.0–3.0** Å range are considered to reflect docking solutions with preserved binding orientation and reasonable conformational overlap with the native structure. Therefore, the obtained RMSD of **2.976** Å confirms that the docking protocol used is moderately accurate and acceptable for further analysis, though minor deviations in certain ligand regions may occur.

Chapter III Results and discussion

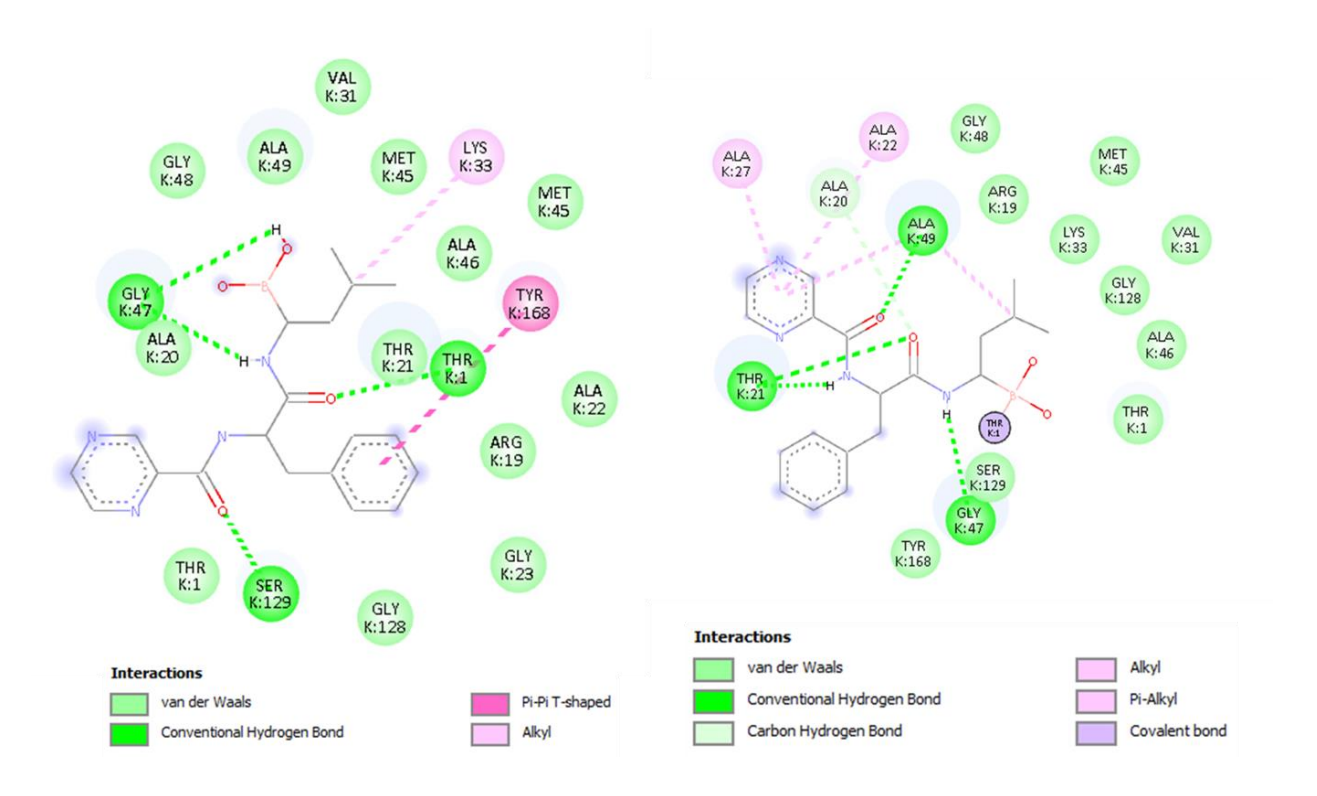


Figure III.2: Docked co-crystallized ligand interaction (left) and Experimental co-crystallized ligand interaction (right)

Figure III.2 presents a comparative analysis of the interaction profiles between the docked ligand (left) and the experimentally co-crystallized ligand (right) within the proteasome binding pocket.

1.1. Common interactions and binding features

Both the docked and experimental structures share van der Waals interactions, notably with hydrophobic residues such as MET 45, ALA 46, and VAL 31, indicating the role of non-polar interactions in stabilizing the ligand within the binding site, and other residues like ARG19, GLY 48 and GLY 128, Their presence in both structures reflects critical regions of molecular recognition and highlights their importance in ligand affinity and specificity.

A significant conventional hydrogen bond interaction is observed with GLY 47 in both cases. This consistent interaction suggests critical anchoring position and supports the hypothesis of electronic complementarity and structural importance of this residue to ligand binding.

Chapter III Results and discussion

1.2 Key differences and structural implications

A significant distinction is the presence of a covalent bond with THR 1 in the experimental structure, which is absent in the docked model. This interaction, likely reversible, implies a more effective and lasting inhibitory effect on the ligand and could signify reactivity or rigidity that cannot be fully predicted through standard docking.

The experimental complex also indicates carbon-hydrogen bonds and Pi-Alkyl interactions, indicating a more advanced molecular geometry and stabilizing forces that contribute to high-affinity binding.

Conversely, the docked ligand only shows a Pi-Pi T-shaped interaction between an aromatic ring of the ligand and an amino acid residue TYR 168, which is absent in the experimental structure. This suggests a possible misorientation or overestimation of aromatic stacking during docking.

Residues such as TYR 168 and LYS 33 are involved in divergence: in the experimental model, these residues form van der Waals bonds, whereas in the docked structure, they present as Pi-Pi T-shaped and Alkyl interactions, respectively. These variations suggest that the docking algorithm may have overestimated the strength or nature of some interactions, leading to slight deviations from the native binding conformation.

2. Interpretation of docking results

Table 01: Molecular docking results.

Molecules	Binding energy	Inhibition Constant, theoretical Ki [Temperature = 298.15 K ⁰]		Top performing
	(kcal/mol)			■ Moderate inhibitor
				Moderate inhibitor
I 4	-8.80	352.53		
I5	-8.71	415.50	nM	Weak inhibitors
II9	-8.31	813.23		
I6	-8.20	976.00		
II10	-8.09	1.18		
II7	-7.98	1.42		
I2	-7.67	2.38		
I 1	-7.63	2.54		
II6	-7.58	2.80		
I3	-7.56	2.87	N	
II1	-7.17	5.53	uM	
BO2	-6.65	13.33		
(Co-crystallized ligand)				
II4	-6.50	17.22		
II11	-6.33	22.84		
II8	-6.24	26.56		
II3	-5.94	44.53		
II2	-5.90	47.61		
II5	-5.87	49.82		

The results of molecular docking are summarized in Table 01, categorizing the ligands based on their binding energy ΔG (kcal/mol) and inhibition constant (Ki) values at a reference temperature of 298.15 K°. These two parameters provide critical insights into the interaction strength and inhibitory potential of each ligand.

2.1. Binding energy (ΔG)

Binding energy (kcal/mol) represents the stability of the ligand-protein complex, with more negative values indicating stronger binding affinity. A highly negative ΔG suggests that the ligand forms energetically favorable interactions with the active site residues, stabilizing the complex [4-6].

2.2. Inhibition constant (Ki)

The inhibition constant (Ki) quantifies the concentration required to inhibit the target by 50%, and lower Ki values indicate higher potency. The relationship between ΔG and Ki is expressed by the thermodynamic equation: ΔG = -RTln(Ki) [7-9].

Where:

 ΔG : Binding free energy (kcal/mol)

R: Gas constant = $1.987 \text{ cal/mol} \cdot \text{K}$

T: Temperature in Kelvin (298.15 K^o)

Ki: Inhibition constant in M

2.3. Ranking and activity profiles

The ligands were ranked based on their binding energy and Ki values, and categorized into three distinct activity profiles: Top-performing inhibitors, Moderate inhibitors, and Weak inhibitors. The categorization is visually represented using a color-coded scheme in Table 01.

The weak inhibitors can be rejected because they have binding energy value less than the cocrystallized ligand value as shown in table 01, where the rest of the ligands demonstrated better predicted binding affinities, suggesting potentially superior inhibitory activity compared to the reference compound.

2.3.1. Top-performing inhibitors

The top-performing inhibitors exhibit strong binding affinity and nanomolar Ki values, reflecting high inhibitory activity. These ligands could be great candidates for further drug development:

- I4 Binding Energy = -8.80 kcal/mol, Ki = 352.53 nM
- I5 Binding Energy = -8.71 kcal/mol, Ki = 415.50 nM
- II9 Binding Energy = -8.31 kcal/mol, Ki = 813.23 nM
- I6 Binding Energy = -8.20 kcal/mol, Ki = 976.00 nM

These ligands demonstrated the most favorable interactions in the binding site, including strong hydrogen bonding, Pi-Pi stacking, and van der Waals contacts, resulting in nanomolar inhibition constants.

2.3.2. Moderate inhibitors

Moderate inhibitors possessed binding energies between -8.09 to -7.17 kcal/mol and Ki values in the micromolar range (1 to 5.53 μ M). Despite their lower affinity compared to the top-performing ligands, these compounds also possess significant binding potential:

II10, II7, I2, I1, II6, I3, II1

These ligands can be employed as starting points for lead optimization, particularly focusing on the optimization of interactions with key residues and minimizing steric clashes.

2.3.3. Weak inhibitors

The remaining compounds, classified as weak inhibitors, showed less favorable binding energies (\geq -6.50 kcal/mol) and high Ki values (> 17 μ M), indicating reduced binding affinity and lower inhibitory potential:

II4, II11, II8, II3, II2, II5

These molecules may lack essential pharmacophores or show suboptimal placement within the binding pocket, leading to weaker interactions and higher Ki values.

3. Comparative analysis of ligand-protein interactions

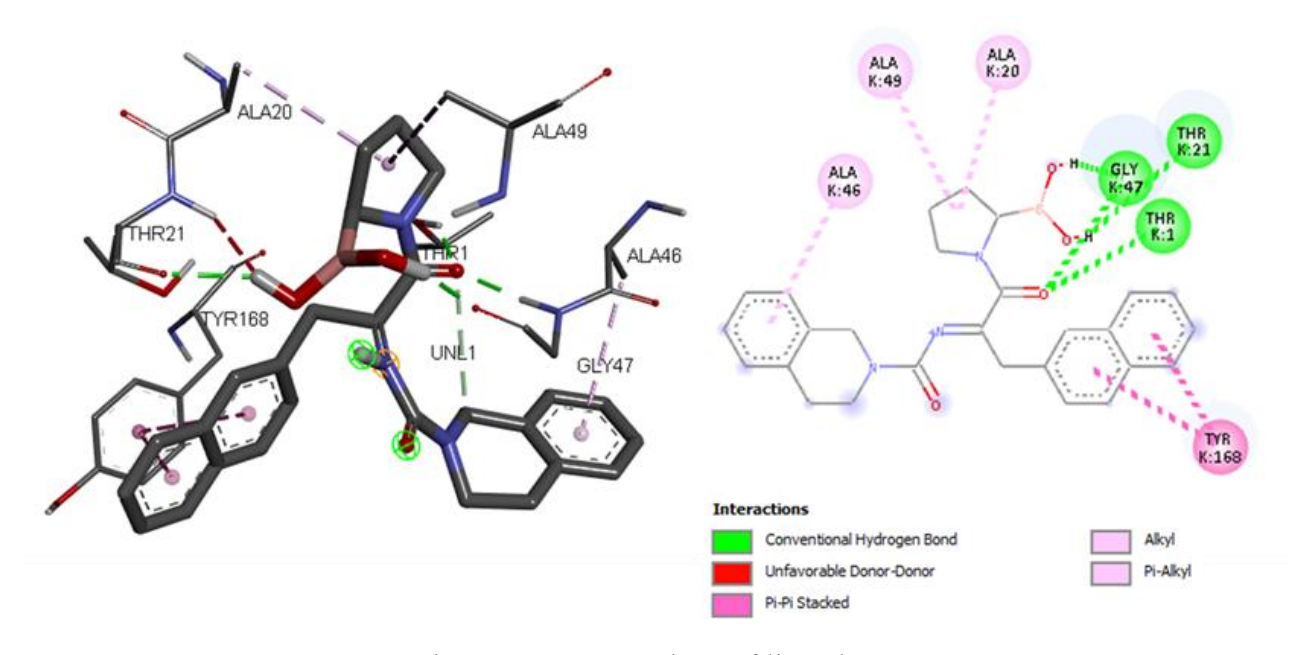


Figure III7: Interactions of ligand I4

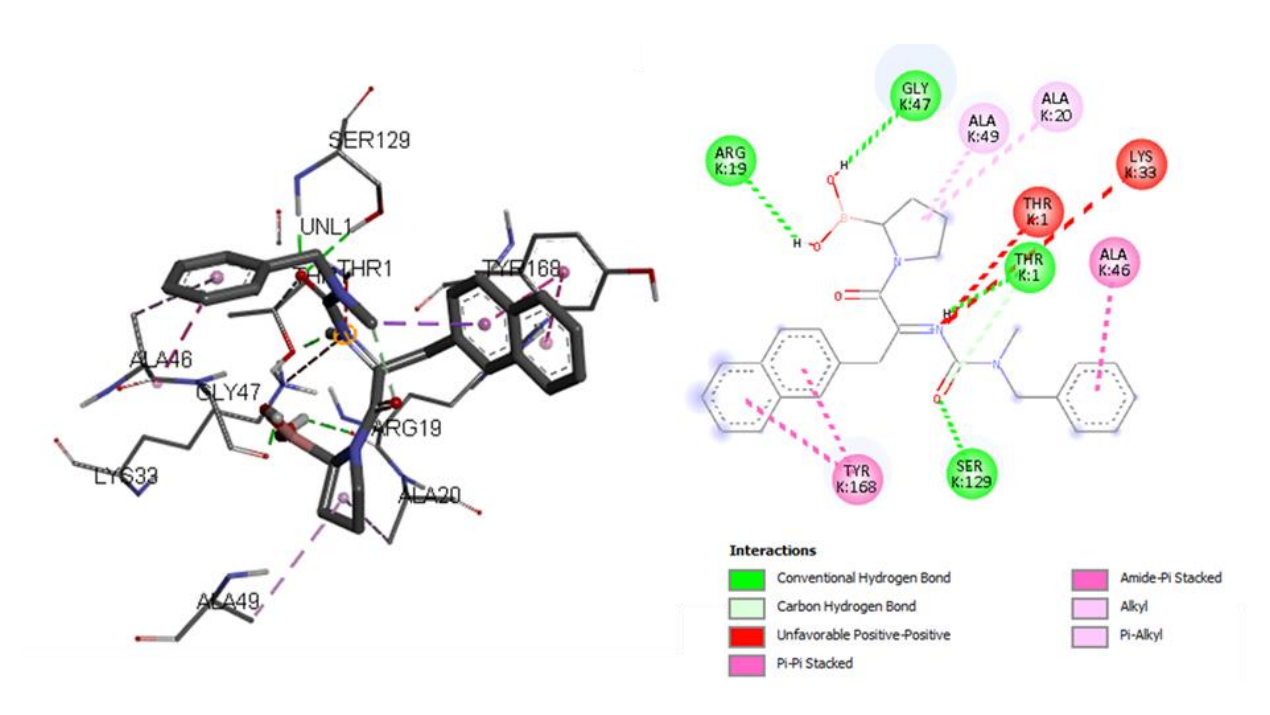


Figure 8: Interactions of ligand I5

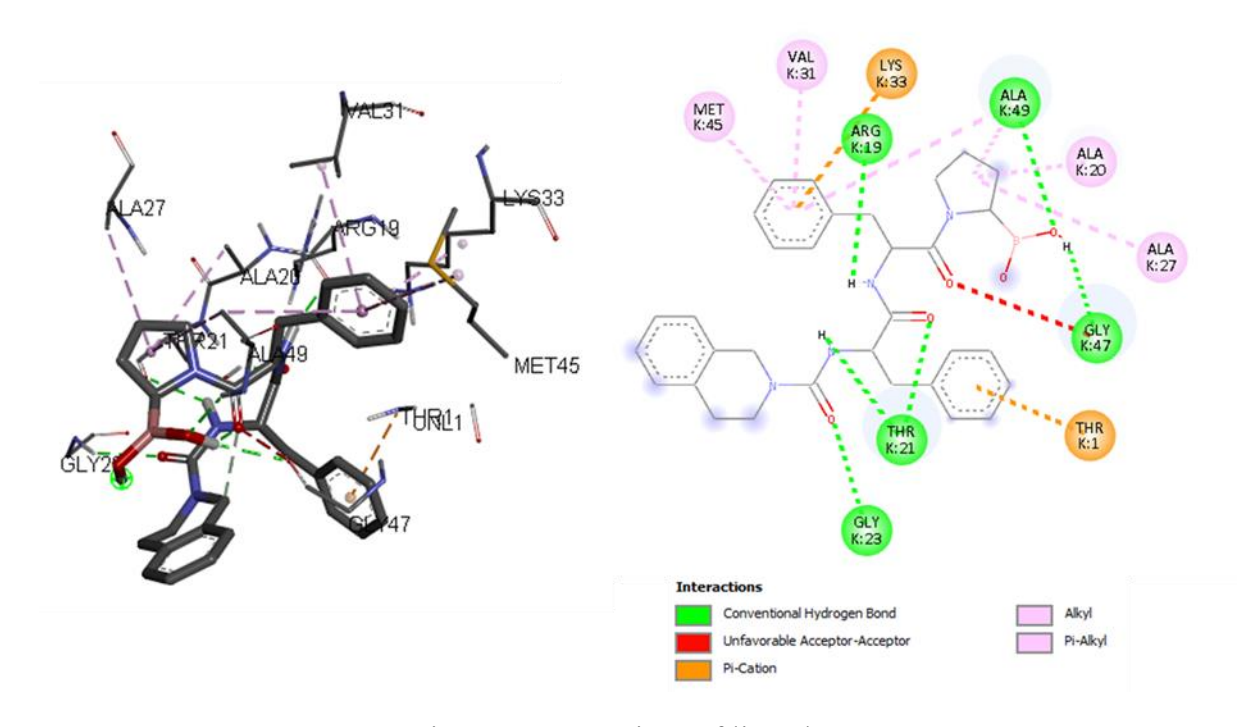


Figure 9: Interactions of ligand II9

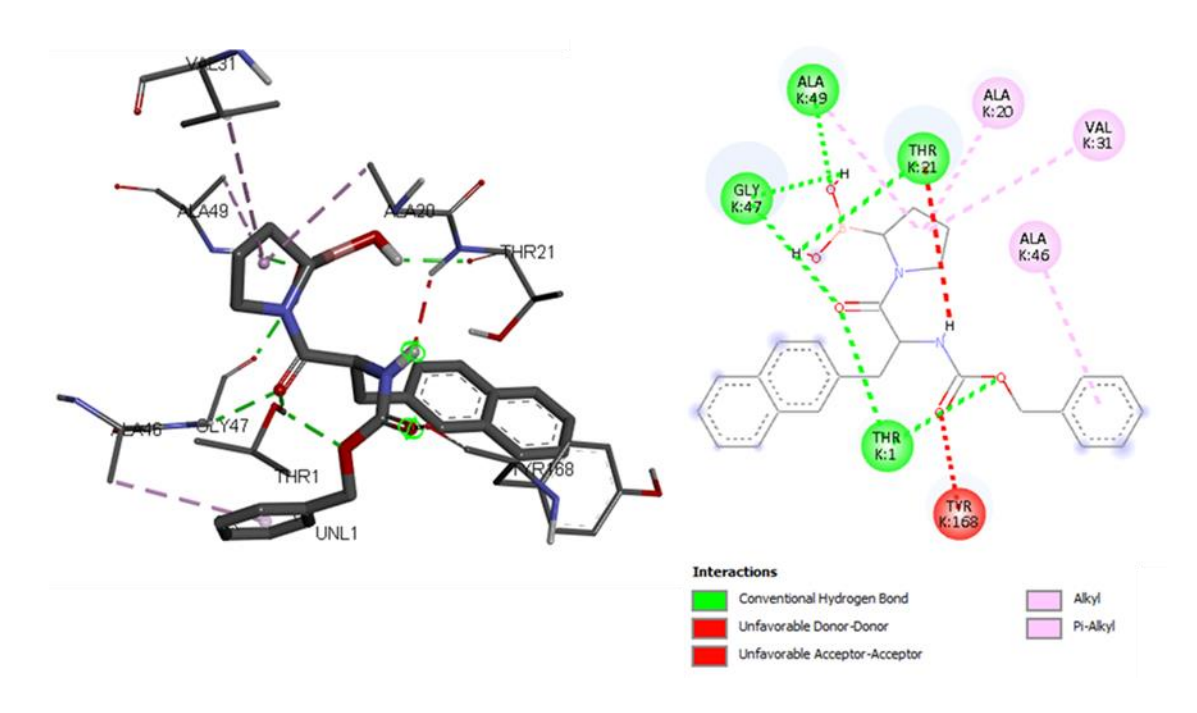


Figure 10: Interactions of ligand I6

This study aimed to investigate the binding affinities and interaction profiles of four selected inhibitors (I4, I5, II9, and I6) against the 20S proteasome (PDB ID: 2F16). Molecular docking analyses were performed to assess how structural variations among the ligands influenced their binding energies (Δ G) and inhibition constants (Ki), identifying critical interactions that contribute to binding efficacy.

3.1. Inhibitor I4: Optimal binding profile

I4 exhibited the strongest binding affinity ($\Delta G = -8.80 \text{ kcal/mol}$; Ki = 352.53 nM), positioning it as the top-performing inhibitor of the selected ligands. The high binding is a consequence of several key interactions:

- **Pi-Pi stacking** with TYR168, a well-aligned aromatic interaction that significantly stabilizes the ligand within the binding pocket [2]. It aligns well with theoretical models emphasizing aromatic stacking as a potent stabilizing force in protein-ligand complexes [10].
- Conventional hydrogen bonds with THR1, THR21, and GLY47, which anchor the ligand and facilitate optimal orientation.

• **Alkyl** with ALA49, ALA20 and **Pi-Alkyl interactions** with ALA26, providing hydrophobic contacts that also support the binding stability.

• **Donor-donor** interaction with THR21, which introduce steric clashes and electrostatic repulsions.

The predominance of stabilizing interactions effectively compensates the repulsive effect of donor-donor interaction, maintaining a balanced orientation and a net favorable binding energy. This is consistent with Kitchen et al [11], who emphasized the importance of steric optimization in virtual screening.

3.2. Inhibitor I5: Strong binding but suboptimal orientation

I5 showed a slightly lower binding affinity ($\Delta G = -8.71 \text{ kcal/mol}$; Ki = 415.50 nM) compared to I4. The interaction pattern of I5 shares similarities with I4, including:

- **Hydrogen bonds** with THR1, GLY47, indicating a well-conserved binding network.
- **Pi-Pi stacked interaction** with TYR168, although slightly misaligned, suggesting a suboptimal aromatic interaction that may reduce stacking stability.

And among the top ranked ligands, I5 uniquely displays a **Carbon hydrogen bond** with THR1 which can contribute to specificity and fine-turning of binding orientation and suggest an additional layer of stabilization.

Amide-Pi stacked with ALA46 plays a key supportive role in stabilizing the binding conformation, it enhances molecular recognition and may help compensate for destabilizing electrostatic clashes in the complex.

Alkyl with ALA49, ALA20 and **Pi-Alkyl interactions** with ALA46, providing hydrophobic contacts that support the binding stability.

A notable **positive-positive interaction** with THR1 and LYS33, potentially leading to electrostatic repulsion, raising the binding energy and partially compromising the stability of the complex.

The presence of a misaligned Pi-Pi interaction, Amide-Pi and hydrogen bonds provide high affinity and specificity. However, the presence of positive-positive conflict may slightly offset

this affinity and indicates that **I5** may require minor structural modifications in order to align its aromatic ring with the TYR168 plane more effectively and optimize its binding performance.

3.3. Inhibitor II9: Unique Pi-Cation interaction but moderate binding

II9 exhibited a moderate binding affinity ($\Delta G = -8.31 \text{ kcal/mol}$; Ki = 813.23 nM). Unlike I4 and I5, II9 lacks significant Pi-Pi stacking interactions with TYR168 which could explain its lower efficacy, instead relying on:

- A **Pi-cation interaction** involving THR1 and LYS33, contributing significant stabilization comparable to Pi-Pi stacking.
- Multiple **hydrogen bonds** with GLY47, GLY23, ALA49, THR21 and ARG19, forming a well-established hydrogen bond network.
- An **unfavorable acceptor-acceptor interaction** where two electronegative groups approach without the mediation of a hydrogen donor (C=O groups of the ligand and GLY47), resulting in electrostatic repulsion and increasing energetic penalty.
- **Alkyl interactions** with ALA20, ALA27 and ALA49, **Pi-Alkyl** with VAL31, ALA49 and MET45, provide hydrophobic stabilization by enhancing the affinity between nonpolar regions of the ligand and surrounding residues that strengthen the ligand-protein binding.

The lack of Pi-Pi stacking and the presence of an unfavorable acceptor-acceptor interaction likely account for the reduced aromatic stabilization and binding efficacy relative to I4 and I5. However, the Pi-cation interaction remains a notable stabilizing feature, suggesting that structural modifications could optimize its interaction geometry.

3.4. Inhibitor I6: Weaker binding and steric clashes

I6 demonstrated the lowest binding affinity among the four inhibitors ($\Delta G = -8.20 \text{ kcal/mol}$; Ki = 976.00 nM). Several factors contribute to its suboptimal binding:

- **Donor-donor interaction** between NH₂ and OH groups of THR21, introducing steric clashes and electrostatic repulsion.
- Acceptor-acceptor interaction between carbonyl group of TYR168 and carbonyl group of the ligand, further destabilizing the complex.

Alkyl interactions with ALA20, ALA49 and VAL31, Pi-Alkyl interactions with ALA46, which provide some hydrophobic stabilization but are less energetically favorable than Pi-Pi stacking.

• **Conventional hydrogen bonds** with GLY47, THR1, THR21 and ALA49, form a strong, directional interaction within the proteasome active site.

The absence of significant Pi-Pi interactions and the presence of multiple unfavorable contacts significantly reduce the binding strength of I6. This ligand may require strategic modifications to minimize steric clashes and align its aromatic ring for potential Pi-Pi stacking.

Table 02: Summary of key insights

Feature	14	15	119	16
Docking Score (kcal/mol)	-8.80	-8.71	-8.31	-8.20
Inhibition Constant (Ki)	352.53 nM	415.50 nM	813.23 nM	976.00 nM
Hydrogen Bonds	GLY47, THR1, THR21	GLY47, THR1, SER129, ARG19	GLY47, ALA49, GLY23, THR21, ARG19	GLY47, THR1 THR21,ALA49
Pi Interactions	-Pi-Pi stacking (TYR168) -Pi-Alkyl (ALA46)	-Pi-Pi stacking (TYR168) -Amide- Pi (ALA46) -Pi-Alkyl (ALA46)	-Pi-Cation (THR1/LYS33) -Pi-Alkyl (VAL31/MET45)	-Pi-Alkyl (ALA46)
Unfavorable Contacts	Donor-Donor	Positive-Positive (THR1/LYS33)	Acceptor- Acceptor (GLY47)	Donor-Donor (THR21), Acceptor- Acceptor (TYR168)
SAR Potential	High	High	Moderate	Low-Moderate

4. Structural and conformational analysis of ligands

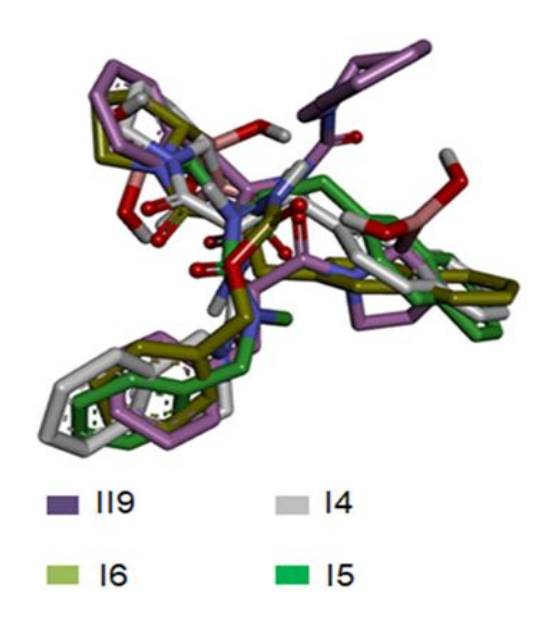


Figure 11: Superposition of the top performing ligands

The superposition analysis of the top-performing ligands (I4, I5, II9, and I6) reveals distinct structural and spatial orientations that help explain the variations in binding affinity and interaction profiles:

- Optimal alignment of I4: The central and well-aligned conformation of I4 within the binding pocket highlights its optimal fit and interaction network.
- Misaligned aromatic systems and partial reorientation of I5 and I6: Despite sharing similar structural frameworks with I4, both I5 and I6 adopt a slightly displaced conformation and that impact binding stability
- Structural limitations of II9 and Steric displacement: The structural alignment of II9 has a steric shift, due to incomplete fit into the active site. The ligand takes a slightly different structure, which may be responsible for its lower binding affinity.

This conformation highlights the influence of ligand rigidity and limited flexibility, which can hinder optimal positioning in the binding site a phenomenon previously described for inhibitors with saturated ring systems [12].

5. Implications for inhibitor optimization

The structural superposition analysis underscores the importance of steric precision and aromatic alignment in inhibitor design. To enhance binding efficacy for compounds like II9 and I6, the following strategies are recommended:

- Aromatic ring modifications: Introduce aromatic cycles to mimic the Pi-Pi interaction observed in I4, potentially reducing the binding energy by 1.0 kcal/mol.
- Polar group modulation: Replace conflicting acceptors to suppress electrostatic repulsion, improving ligand orientation.
- Molecular dynamics simulations: Conduct MD simulations to assess the impact of RMSD (2.976 Å) on ligand flexibility and binding stability, validating structural predictions [13].

These optimization strategies are inspired by recent advanced practices in structure-based drug design, where simulations guided refinement is employed to maximize binding efficacy [14].

Bibliography

[1] Ramírez, D.; Caballero, J. Is It Reliable to Take the Molecular Docking Top Scoring Position as the Best Solution without Considering Available Structural Data Molecules 2018, 23 (5), 1038. https://doi.org/10.3390/molecules23051038.

- [2] Alandijany, T. A.; El-Daly, M. M.; Tolah, A. M.; Bajrai, L. H.; Khateb, A. M.; Alsaady, I. M.; Altwaim, S. A.; Dubey, A.; Dwivedi, V. D.; Azhar, E. I. Investigating the Mechanism of Action of Anti-Dengue Compounds as Potential Binders of Zika Virus RNA-Dependent RNA Polymerase. *Viruses* 2023, 15 (7), 1501. https://doi.org/10.3390/v15071501.
- [3] Aruwa, C. E.; Dweba, Y.; Ayodele, O. M.; Sabiu, S. Modulating Acinetobacter baumannii BfmR (RstA) Drug Target: Daniellia oliveri Compounds as RstA Quorum Sensing Inhibitors. Comput. Biol. Chem. 2025, 117, 108413.https://doi.org/10.1016/j.compbiolchem .2025.108413.
- [4] Cozzini, P., Fornabaio, M., Marabotti, A., Abraham, D. J., Kellogg, G. E., & Mozzarelli, A. (2002). Simple, intuitive calculations of free energy of binding for protein–ligand complexes. 1. Models without explicit constrained water. Journal of Medicinal Chemistry, 45(9), 1952–1963. https://doi.org/10.1021/jm0200299
- [5] Jiménez, J. S., & Benítez, M. C. (2024). Gibbs free energy and enthalpy–entropy compensation in protein–ligand interactions. Biophysica, 4(2), 21. https://doi.org/10.3390/biophysica4020021
- [6] Dullweber, F., Sevenich, F. W., & Klebe, G. (2000). Determination of accurate thermodynamics of binding for proteinase-inhibitor interactions. In G. A. Press (Ed.), Drug Design and Discovery (pp. 863–876). Springer. https://doi.org/10.1007/978-1-4615-4141-7 134
- [7] Darras, F. H., & Pang, Y. P. (2017). On the use of the experimentally determined enzyme inhibition constant as a measure of absolute binding affinity. Biochemical and Biophysical Research Communications, 489(1), 17–20. https://doi.org/10.1016/j.bbrc.2017.05.168
- [8] Cheng, Y., Slon-Usakiewicz, J. J., Wang, J., Purisima, E. O., & Konishi, Y. (1997). Thermodynamic investigation of enzyme and inhibitor interactions with high affinity. In Techniques in Protein Chemistry (Vol. 8, pp. 355–364). Academic Press. https://doi.org/10.1016/S1080-8914(97)80051-8.

[9] Borea, P. A., Varani, K., Merighi, S., Piaz, A. D., Gilli, P., & Gilli, G. (2003). Receptor binding thermodynamics at the neuronal nicotinic receptor. Current Topics in Medicinal Chemistry, 3(13), 1335–1344. https://doi.org/10.2174/1568026043451410.

- [10] Leach, A. R. (2001). Molecular modelling: Principles and applications (2nd ed.). Pearson Education.
- [11] Kitchen, D. B., Decornez, H., Furr, J. R., & Bajorath, J. (2004). Docking and scoring in virtual screening for drug discovery: Methods and applications. Nature Reviews Drug Discovery, 3(11), 935–949. https://doi.org/10.1038/nrd1549.
- [12] Bissantz, C., et al. (2000). Journal of Medicinal Chemistry, 43(25), 4759–4767.
- [13] Karplus, M., & McCammon, J. A. (2002). Molecular dynamics simulations of biomolecules. Nature Structural Biology, 9(9), 646–652. https://doi.org/10.1038/nsb0902-646.
- [14] Sliwoski, G., et al. (2014). Pharmacological Reviews, 66(1), 334–395.



Genaral conclusion

This in silico study evaluated the inhibitory activity of 17 bioactive peptides targeting the 20S proteasome (PDB ID: 2F16) using molecular docking using AutoDock. The docking procedure was validated by an acceptable RMSD value of 2.976 Å, which confirmed the methodological robustness of the simulation and revealed significant information on ligand-receptor interactions. The peptides were ranked according to their binding energy and inhibition constant (Ki), leading to the identification of four top-performing ligands I4, I5, II9, and I6 each with distinct interaction profiles and structural features.

Docking the co-crystallized ligand highlighted discrepancies between computational and experimental results. While only the experimental ligand formed a covalent bond, indicating a more rigid and reversible inhibition mode that docking methods typically fail to reproduce due to methodological limitations. A Pi-Pi stacking was observed only in docked ligand but both shared van der Waals interactions and hydrogen bonding with Gly47, emphasizing its critical role in ligand recognition. This suggests that non-covalent interactions (such as van der waals, hydrogen bonds) are well-predicted by docking, but covalent binding requires special protocols.

A detailed analysis of binding modes indicated that all top ligands possessed multiple van der Waals interactions and hydrogen bonds like with Gly47, a residue consistently implicated in stabilizing ligand—proteasome binding. Notably, I4 and I5 exhibited pi-pi stacked interactions with TYR168, which enhance binding affinity through aromatic ring stabilization. However, these ligands also had destabilizing factors: I4 showed an unfavorable donor-donor interaction, while I5 presented a positive-positive electrostatic clash which could lead to local repulsion, and decrease binding efficiency and stability.

The ligand II9 benefited from a pi-cation interaction, a known stabilizing electrostatic process, but this was balanced by an unfavorable acceptor-acceptor interaction that might disrupt local geometry. I6, despite displaying the lowest binding energy, was characterized by both donor-donor and acceptor-acceptor clashes, which likely compromise its conformational stability and reduce its functional binding affinity

Genaral conclusion

Besides, conformational superposition of the top four ligands showed nearly identical conformations, with only minimal positional variations due to differences in side-chain flexibility or electrostatic environments, reflecting the proteasome active site's adaptability to structurally similar ligands

Based on these findings, we propose several optimization strategies. Unfavorable electrostatic (donor-donor, acceptor-acceptor, and positive-positive) should be addressed by rational ligand modification. Enhancing favorable interactions particularly hydrogen bonding interactions, Pi-Pi stacking with TYR168 and Pi-cation contacts may increase binding stability. While covalent bonding remains beyond the capability of classical docking, its imitation by more effective non-covalent interactions could be a promising avenue. Finally, molecular dynamics simulations and in vitro validation are essential next steps to assess the dynamic performance and biological efficacy of the lead compounds.

In conclusion, this work highlights the promise of bioactive peptides as proteasome inhibitors and the value of computational screening when integrated with structural analysis and rational design. The identified peptides, especially I4, provide a good starting point for further development of selective and efficient proteasome-targeting therapeutics.

Abstract

The ubiquitin-proteasome system (UPS) is a critical regulator of protein degradation, making it a promising target for cancer therapy. This study employed a virtual screening strategy using molecular docking to assess the inhibitory potential of 17 bioactive peptides against the proteasome (PDB ID: 2F16). Ligand structures were optimized in HyperChem and prepared for docking using AutoDock4, enabling the prediction of binding affinities (ΔG) and inhibition constants (Ki).

The virtual screening identified I4 as the top-performing inhibitor ($\Delta G = -8.80 \text{ kcal/mol}$, Ki = 352.53 nM), characterized by Pi-Pi stacking with TYR168 and multiple hydrogen bonds with THR1 and GLY47. In contrast, I6 exhibited weaker binding ($\Delta G = -8.20 \text{ kcal/mol}$, Ki = 976.00 nM), due to steric clashes and donor-donor, acceptor-acceptor conflict that reduced stability.

The findings demonstrate the effectiveness of the virtual screening strategy in prioritizing structurally promising peptide inhibitors, emphasizing the significance of aromatic stacking, hydrogen bonding, and hydrophobic contacts in stabilizing ligand-proteasome interactions. These results provide a basis for further structural optimization and in vitro validation.

Keywords: Proteasome inhibition, Virtual screening, Molecular docking, Bioactive peptides and Binding affinity (ΔG)

<u>Résumé</u>

Le système ubiquitine-protéasome (UPS) est un régulateur essentiel de la dégradation des protéines, ce qui en fait une cible prometteuse pour le traitement du cancer. Cette étude a utilisé une stratégie de criblage virtuel par docking moléculaire pour évaluer le potentiel inhibiteur de 17 peptides bioactifs contre le protéasome (PDB ID : 2F16). Les structures des ligands ont été optimisées dans HyperChem et préparées pour le docking à l'aide d'AutoDock4, permettant ainsi de prédire les affinités de liaison (ΔG) et les constantes d'inhibition (Ki).

Le criblage virtuel a identifié I4 comme l'inhibiteur le plus performant ($\Delta G = -8,80 \text{ kcal/mol}$, Ki = 352,53 nM), caractérisé par interaction Pi-Pi avec TYR168 et des liaisons hydrogène avec THR1 et GLY47. En revanche, I6 a montré une liaison plus faible ($\Delta G = -8,20 \text{ kcal/mol}$, Ki = 976,00 nM), en raison de conflits stériques et d'interactions donneur-donneur et accepteur-accepteur qui ont réduit la stabilité.

Les résultats démontrent l'efficacité de la stratégie de criblage virtuel pour prioriser les inhibiteurs peptidiques potentiels, en soulignant l'importance de l'empilement aromatique, des liaisons hydrogène et des contacts hydrophobes dans la stabilisation des interactions ligand-protéasome. Ces résultats constituent une base pour des optimisations structurelles et des validations in vitro.

Mots-clés : Inhibition du protéasome, Criblage virtuel, Docking moléculaire, Peptides bioactifs, Affinité de liaison (ΔG)